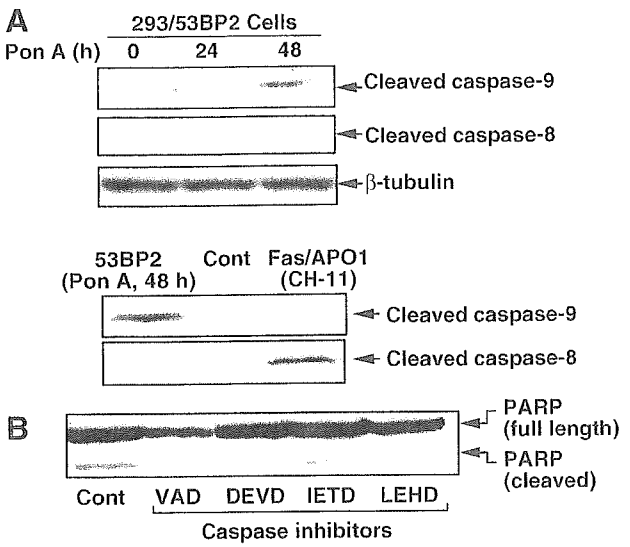

Figure 5 Involvement of caspase-9 in apoptosis induced by 53BP2S. (A) Activation of caspase-9 by 53BP2S. 293/53BP2 cells were treated by pon A (5 μM) for the indicated periods (h). Each cell lysate (10 μg protein) was examined for the activated ('cleaved') form of caspase-9 by Western blotting with anti-caspase-9 (cleaved form) or anti-caspase-8 (cleaved form) antibodies (upper panel). β-tubulin was used as an internal control. In the lower panel, 293/53BP2 cells were either stimulated with the agonistic anti-Fas antibody (CH-11) or treated with pon A and the activation of caspase-8 or caspase-9 was similarly examined. (B) Inhibition of the PARP cleavage by caspase inhibitors. 293/53BP2 cells were cultured with or without caspase inhibitors for 12 h and treated with pon A (5 μM) for 48 h. The cell lysate was prepared and examined for the PARP cleavage by Western blotting. The same amounts of each cell lysate (10 μg protein) were analyzed. Cont, DMSO alone; VAD, common inhibitor for the caspase-family (Z-VAD-FMK); DEVD, caspase-3-specific inhibitor (Z-DEVD-FMK); IETD, caspase-8-specific inhibitor (Z-IETD-FMK); LEHD, caspase-9-specific inhibitor (Z-IETD-FMK).

was diminished, indicating a decrease in $\Delta\Psi$m. In contrast, no such changes were observed in the control cells transfected with pEGFP. In Fig. 4B, the temporal change of $\Delta\Psi$m in 293/53BP2 cells is shown. When 53BP2S was expressed, progressive reduction of $\Delta\Psi$m detected by the rhodamine123 fluorescence intensity was observed over time, concomitantly with the appearance of apoptotic cells (compare with Fig. 2B). No such change was observed in control 293/LZ cells.

Involvement of caspase-9 in apoptosis induced by 53BP2S

Finally, to examine the upstream caspase cascade involved in the 53BP2S-mediated apoptosis, 293/53BP2 cell lysates were prepared after 24 and 48 h of pon A treatment. The presence of activated (cleaved) forms of caspase-8 and caspase-9 were examined in these cells. Figure 5A shows that caspase-9, but not caspase-8, was activated following the induction of 53BP2S. To confirm these observations, the effects of specific inhibitors for caspase-3, -8, and -9 were examined. As shown in Fig. 5B, the effects of peptide inhibitors among all types of known caspases (VAD), caspase-3 (DEVD), caspase-8 (IETD) and caspase-9 (LEHD) were shown. Although VAD, DEVD and LEHD effectively blocked the PARP cleavage induced by 53BP2S, only a minimal effect was observed with IETD. These findings indicate that 53BP2S induces apoptosis through the mitochondrial ('intrinsic') death pathway.

Discussion

The present data have revealed the involvement of mitochondria in the 53BP2-mediated apoptosis. 53BP2 has two protein isoforms, 53BP2S and 53BP2L, generated by alternative splicing (Takahashi *et al.* 2004). These two 53BP2 proteins are localized predominantly in the cytoplasm and exhibited similar biological actions although we do not currently know the reason of such redundancy. In this study, we have explored the proapoptotic action of 53BP2S using transient expression and the stable cell line in which 53BP2 is under the stringent control of pon A. When expressed, 53BP2S was located in the mitochondria and induced cell death associated with $\Delta\Psi$m repression, caspase-9 activation, PARP cleavage, annexin V staining, and typical nuclear morphology, suggesting the involvement of intrinsic death pathway.

Regarding the possible involvement of 53BP2 in the cellular response to DNA damage, we have previously reported the positive correlation between the level of 53BP2 mRNA expression and the sensitivity to DNA damaging agents in various human cancer cell lines although no mutation of 53BP2 gene was detected (Mori *et al.* 2000). In addition, Ao *et al.* (2001) found that 53BP2S expression augmented the cellular apoptotic response to the DNA damage. Lopez *et al.* (2000) observed that the DNA damage induced the 53BP2 expression and protein stabilization leading to apoptosis. Bergamaschi *et al.* (2004) recently reported similar observations with ASPP2 (53BP2L). Therefore, it is likely that the activated p53 may augment the 53BP2-mediated cell death. In support of this action of p53, Marchenko *et al.* (2000) demonstrated the mitochondrial translocation of p53 upon irradiation and induction of apoptosis through the intrinsic death pathway. Mihara *et al.* (2003) further explored the mitochondrial involvement of p53 and found that p53 formed a complex with

Bcl-2 and $BclX_L$ followed by permeabilization of the outer mitochondrial membrane.

Intriguingly, Iwabuchi *et al.* (1998) and Samuels-Lev *et al.* (2001) found that p53-mediated transactivation was augmented by 53BP2S and 53BP2L (ASPP2), respectively. Samuels-Lev *et al.* (2001) proposed a model that 53BP2L interacts with p53 in the nucleus and specifically enhances gene expression of p53 responsive pro-apoptotic genes such as Bax. Although the 3D structure model of p53 and 53BP2 complex (Gorina & Pavletich 1996) does not support their hypothesis because when 53BP2 binds to p53, it involves the L3 loop of p53 (required for its DNA binding) and the H1 helix (required for p53 dimerization), thus precluding the p53 binding to DNA, there may be multiple mechanisms by which 53BP2 induces apoptosis.

In addition to the possible involvement of p53 and 53BP2 in apoptosis, 53BP2 abnormality is implicated in autoimmunity such as systemic lupus erythematosus (SLE) since one of the genetic loci of the familial incidence of SLE was shown to be located to 1q42.1 (Tsao *et al.* 1997), to which *TP53BP2* is located (Yang *et al.* 1997). This is coincided with the fact that abnormalities of various apoptosis-associated factors were reported in SLE and its animal models (Fisher *et al.* 1995; Sneller *et al.* 1997; Jackson & Puck 1999). Further genetic studies are needed to find a link between 53BP2 and autoimmunity.

Our observations together with those of others suggest that 53BP2 is involved in apoptosis at multiple steps and is implicated in various pathological processes. Since 53BP2 has been shown to interact with a number of proteins responsible for the regulation of apoptosis such as p53, Bcl-2 and NF-κB p65 subunit, selective interaction of 53BP2 with these proteins may determine the susceptibility of cells to trigger the apoptotic pathway.

Experimental procedures

Reagents and antibodies

FuGENE 6 and SuperFect transfection reagents were purchased from Roche Molecular Biochemicals (Indianapolis, IN, USA) and QIAGEN (Qiagen Inc., Valencia, CA, USA), respectively. PE-conjugated annexin V and 7-AAD (Becton Dickenson, Mountain View, CA, USA), ponasterone A (pon A) (Invitrogen, La Jolla, CA, USA) were commercially obtained. The caspase inhibitors (caspase-3 inhibitor, Z-DEVD-FMK; caspase-8 inhibitor, Z-IETD-FMK; caspase-9 inhibitor, Z-LEHD-FMK; caspase-family inhibitor, Z-VAD-FMK) were purchased from MBL. Mouse monoclonal antibodies to human 53BP2 (BD Transduction Laboratories, San Diego, CA, USA), β-tubulin (Sigma Chemical Co., St. Louis, MO, USA), human lactate dehydrogenase (LDH) (MBL, Nagoya, Japan) and human Fas (Sigma), and mouse polyclonal antibody to human mitochondrial heat shock protein 70 (Affinity Bioreagents, Golden, CO, USA) were purchased from individual suppliers. The rabbit polyclonal antibody to human 53BP2 was a generous gift from L. Naumovski (Stanford University, CA, USA). Mouse monoclonal antibodies to caspase-8 (cleaved form) and caspase-9 (cleaved form) and rabbit polyclonal antibody to PARP were purchased from Cell Signaling Technology (Beverly, MA, USA).

Plasmids

Construction of the 53BP2S expression plasmids, pcDNA3.1–53BP2 and pEGFP-53BP2, expressing 53BP2S protein (1005 amino acids) either alone or in fusion with green fluorescence protein (GFP), was reported previously (Yang *et al.* 1999). pCEP4-ASPP2, expressing 53BP2L (1128 amino acids), was a gift from L. Naumovski. pDsRed2-Mito, expressing a fusion protein of the *Discosoma* sp. red fluorescent protein linked to the mitochondrial targeting sequence from subunit VIII of human cytochrome oxidase, was purchased from BD Bioscience Clontech (Palo Alto, CA, USA).

Cell lines and cultures

The 53BP2S inducible cell line 293/53BP2 and its control cell line 293/LZ were kindly provided by Charles D. Lopez, Stanford University, CA, USA and previously described (Lopez *et al.* 2000). These cells were grown at 37 °C in 5% CO_2 in Dulbecco's modified Eagle medium (DMEM) with 10% (v/v) heat-inactivated foetal calf serum, 290 μg/mL of L-glutamine, 100 U/mL penicillin, 100 μg/mL streptomycin, 600 μg/mL G418 and 500 μg/mL Zeocin. The parental 293 and HeLa cells were grown at 37 °C in DMEM with 10% (v/v) heat-inactivated foetal calf serum (IBL, Maebashi, Japan), 1 mM glutamate, 100 U/mL penicillin, and 100 μg/mL streptomycin. A human pancreatic cancer cell line MIA PaCa-2 was grown in Eagle minimal essential medium supplemented with nonessential amino acids, 10% (v/v) heat-inactivated foetal calf serum, 100 U/mL penicillin, and 100 μg/mL streptomycin.

Immunostaining

Semi-confluent MIA PaCa-2 cells on Laboratory-Tek tissue culture chamber slides were fixed with 4.5%

paraformaldehyde in PBS for 15 min at room temperature, rinsed twice with PBS, and incubated with PBS containing 0.5% Triton X-100 for 20 min at room temperature. They were subsequently incubated with the primary anti-53BP2 mouse antibody (B92320, Transduction Laboratories, Lexington, KY, USA) for 1 h at 37 °C, rinsed three times with PBS containing 0.05% Triton X-100, and incubated with the secondary antibody, rhodamine-conjugated goat anti-mouse IgG (Calbiochem-Novabiochem, La Jolla, CA, USA), for 1 h at 37 °C. The slides were rinsed with PBS three times and mounted with buffered glycerol for fluorescent microscopic examination. Primary and secondary antibodies were diluted at 1 : 100 and 1 : 200, respectively, in PBS containing 3% bovine serum albumin.

Cell fractionation

In order to examine the cellular localization of 53BP2 in the 293/53BP2 cells, cells were pretreated with pon A (5 μM, 48 h) and subjected to fractionation using commercial kits (Nuclear/Cytosol Fractionation Kit and Mitochondria/Cytosol Fractionation Kit, BioVision, Mountain View, CA, USA). The heavy membrane precipitate containing mitochondria was extensively washed in order to avoid the contamination of cytoplasmic proteins. The identification of 53BP2 and validation of cell fractionation were performed by Western blotting with antibodies to 53BP2, LDH (cytoplasmic marker) and mitochondrial heat shock protein 70 (mitochondria marker).

Flow cytometric analysis of apoptosis

In order to assess apoptosis, flow cytometric analysis was performed using FACScan (Becton Dickinson). MIA PaCa-2 cells were transiently transfected with pcDNA3.1–53BP2 expressing 53BP2S or pCEP4-ASPP2 expressing 53BP2L using SuperFect according to the manufacturer's recommendations. Cells at a concentration of approximately 1×10^6 cells/mL were washed twice with cold PBS and resuspended in annexin V binding buffer (10 mM HEPES-NaOH (pH 7.4), 140 mM NaCl and 2.5 mM $CaCl_2$). In some experiments, cells were double-stained with annexinV and 7-Amino-actinomycin D (7-AAD). 293/53BP2 cells were induced to express 53BP2 by incubation with 5 μM pon A and apoptotic cells were similarly counted.

Microscopic examination

In order to examine the cellular localization of 53BP2S, 293 cells were cultured on 2-well Laboratory-Tek tissue culture chamber slides and transfected with 0.4 μg of pEGFP-53BP2 expressing 53BP2S together with 0.1 μg of the mitochondria targeting plasmid, pDsRed2-Mito (BD Bioscience Clontech). The transfected cells were fixed with 4.0% paraformaldehyde in PBS for 15 min at room temperature, and observed under the confocal microscope (RADIANCE2000; Bio-Rad, Hercules, CA, USA). Each fluorophore was recorded separately using narrow-band filters centered at 522 nm for GFP fluorescence and 605 nm for DsRed2 fluorescence.

Evaluation of apoptosis by Western blotting

Apoptosis was also assessed by the cleavage of PARP, and caspases-8 and -9 by Western blotting using relevant antibodies described above. Briefly, whole cell extracts were lyzed in 200 μL of ice-cold lysis buffer (50 mM Tris-HCl (pH 8.0), 100 mM NaCl, 5 mM EDTA, 50 mM sodium fluoride, 2 mM dithiothreitol, 0.25% Nonidet P-40, 1 mM phenylmethyl-sulfonyl fluoride, 10 μg/mL aprotinin, 10 μg/mL leupeptin and 1 μg/mL pepstatin (A). The lysate was cleared by centrifugation and the protein concentration of the whole cell extract was measured using Bio-Rad DC protein assay kit (Bio-Rad). Equal amounts of cell lysates (10 μg protein) were resolved by 10% SDS-PAGE and transferred on nitrocellulose membrane followed by incubating with individual antibodies. The immunoreactive proteins were visualized by ECL.

Determination of mitochondrial $\Delta\Psi$m in cultured cells

To evaluate $\Delta\Psi$m, cells were treated with 10 μg/mL Rh123 for 15 min at 37 °C. After incubation, cells were washed with PBS(+) three times, resuspended in PBS(+), and fluorescence was scored immediately by flow cytometer. To visualize the cells with depressed $\Delta\Psi$m, cells growing on Laboratory-*Tek*II chambered cover glass were stained with 40 nM CMXRos in PBS(+) for 15 min, washed with PBS(+) three times and observed under the confocal microscope (Bio-Rad MRC600UVF). The acquisitions of the mitochondrial images were provided by 585LP emission filter with same setting (Iris: 2.0, Gain: 1.4).

Acknowledgments

We thank Dr Louie Naumovski (Stanford University) for his generous gifts of 293/53BP2 cells, polyclonal antibody to 53BP2, and a plasmid expressing 53BP2L. This work was supported in part by grants-in-aid from the Ministry of Health, Labor and Welfare, the

Ministry of Education, Culture, Sports, Science and Technology of Japan and Japanese Human Sciences Foundation.

References

Ao, Y., Rohde, L.H. & Naumovski, L. (2001) p53-interacting protein 53BP2 inhibits clonogenic survival and sensitizes cells to doxorubicin but not paclitaxel-induced apoptosis. *Oncogene* **20**, 2720–2725.

Bergamaschi, D., Samuels, Y., Jin, B., Duraisingham, S., Crook, T. & Lu, X. (2004) ASPP1 and ASPP2: Common activators of p53 family members. *Mol. Cell. Biol.* **24**, 1341–1350.

Daniel, N.N. & Korsmeyer, S.J. (2004) Cell death: Critical control points. *Cell* **116**, 205–219.

Fisher, G.H., Rosenberg, F.J., Straus, S.E., *et al.* (1995) Dominant interfering Fas gene mutations impair apoptosis in a human autoimmune lymphoproliferative syndrome. *Cell* **81**, 935–946.

Gorina, S. & Pavletich, N.P. (1996) Structure of the p53 tumor suppressor bound to the ankyrin and SH3 domains of 53BP2. *Science* **274**, 1001–1005.

Green, D.R. & Reed, J.C. (1998) Mitochondria and apoptosis. *Science* **281**, 1309–1312.

Iwabuchi, K., Bartel, P.L., Li, B., Marraccino, R. & Fields, S. (1994) Two cellular proteins that bind to wild-type but not mutant p53. *Proc. Natl. Acad. Sci. USA* **91**, 6098–6102.

Iwabuchi, K., Li, B., Massa, H.F., Trask, B.J., Date, T. & Fields, S. (1998) Stimulation of p53-meditated transcriptional activation by the p53-binding proteins, 53BP1 and 53BP2. *J. Biol. Chem.* **273**, 26061–26068.

Jackson, C.E. & Puck, J.M. (1999) Autoimmune lymphoproliferative sundrome, a disorder of apoptosis. *Curr. Opin. Pediatr.* **11**, 521–527.

Judith, H.M., Caroline, D., Jean, C.M. & James, D. (2004) Role of mitochondrial membrane permeabilization in apoptosis and cancer. *Oncogene* **23**, 2850–2860.

Lopez, C.D., Ao, Y., Rohde, L.H., *et al.* (2000) Proapoptotic p53-interacting protein 53BP2 is induced by UV irradiation but suppressed by p53. *Mol. Cell. Biol.* **20**, 8018–8025.

Marchenko, N.D., Zaika, A. & Moll, U.M. (2000) Death signal-induced localization of p53 protein to mitochondria. A potential role in apoptotic signaling. *J. Biol. Chem.* **275**, 16202–16212.

Mihara, M., Erster, S., Zaika, A., *et al.* (2003) p53 has a direct apoptogenic role at the mitochondria. *Mol. Cell* **11**, 577–590.

Mori, T., Okamoto, H., Takahashi, N., Ueda, R. & Okamoto, T. (2000) Aberrant overexpression of 53BP2 mRNA in lung cancer cell lines. *FEBS Lett.* **465**, 124–128.

Naumovski, L. & Cleary, M.L. (1996) The p53-binding protein 53BP2 also interacts with Bc12 and impedes cell cycle progression at G2/M. *Mol. Cell. Biol.* **16**, 3884–3892.

Samuels-Lev, Y., O'Connor, D.J., Bergamaschi, D., *et al.* (2001) ASPP proteins specifically stimulate the apoptotic function of p53. *Mol. Cell* **8**, 781–794.

Sneller, M.C., Wang, J., Dale, J.K., *et al.* (1997) Clinical, immunologic, and genetic features of an autoimmune lymphoproliferative syndrome associated with abnormal lymphocyte apoptosis. *Blood* **89**, 1341–1348.

Takahashi, N., Kobayashi, S., Jiang, X., *et al.* (2004) Expression of 53BP2 and ASPP2 proteins from TP53BP2 gene by alternative splicing. *Biochem. Biophys. Res. Commun.* **315**, 434–438.

Tsao, B.P., Canto, R.M., Kalunian, K.C., *et al.* (1997) Evidence for linkage of a candidate chromosome 1 region to human systemic lupus erythematosus. *J. Clin. Invest.* **99**, 725–731.

Yang, J.P., Ono, T., Sonta, S., Kawabe, T. & Okamoto, T. (1997) Assignment of p53 binding protein (TP53BP2) to human chromosome band 1q42.1 by in situ hybridization. *Cytogenet. Cell Genet.* **78**, 61–62.

Yang, J.P., Hori, M., Takahashi, N., Kawabe, T., Kato, H. & Okamoto, T. (1999) NF-κB subunit p65 binds to 53BP2 and inhibits cell death induced by 53BP2. *Oncogene* **18**, 5177–5186.

Received: 8 October 2004
Accepted: 12 December 2004

ELSEVIER

Journal of Immunological Methods 299 (2005) 189–198

JIM
Journal of
Immunological Methods

www.elsevier.com/locate/jim

Research paper

Establishment of a simple and quantitative immunospot assay for detecting anti-type II collagen antibody using an infrared fluorescence imaging system (IFIS)

Shusuke Ota[a,b], Satoshi Kanazawa[a], Masaaki Kobayashi[b], Takanobu Otsuka[b], Takashi Okamoto[a,*]

[a]*Department of Molecular and Cellular Biology, Nagoya City University Graduate School of Medical Sciences, 1 Kawasumi, Mizuho-cho, Mizuho-ku, Nagoya 467-8601, Japan*

[b]*Department of Musculoskeletal Medicine, Nagoya City University Graduate School of Medical Sciences, 1 Kawasumi, Mizuho-cho, Mizuho-ku, Nagoya 467-8601, Japan*

Received 4 August 2004; received in revised form 29 November 2004; accepted 10 March 2005
Available online 7 April 2005

Abstract

Antibodies to type II collagen (col II) have been detected in patients with rheumatoid arthritis and in animal models of collagen induced arthritis. Here, we describe a novel method to detect anti-col II antibodies using an immunospot assay with an infrared fluorescence imaging system. This method showed very high sensitivity and specificity, and was simple, with low background levels. It also showed higher reproducibility and linearity, with a dynamic range of approximately 500-fold, than the conventional immunospot assay with enhanced chemiluminescence detection. Using this method we were able to demonstrate the antibody affinity maturation process in mice immunized with col II. In these immunized mice, although cross-reactive antibodies reacting with other collagen species were detected in earlier stages of immunization, the titers of cross-reactive antibodies rapidly diminished after the antigen boost, concomitantly with the elevation of the anti-col II antibody. The method and its possible applications are discussed.

Keywords: Infrared imaging system; Collagen-induced arthritis; Anti-type II collagen antibody; Affinity maturation; Rheumatoid arthritis

1. Introduction

Antibodies to type II collagen (col II) have been detected in patients with rheumatoid arthritis (RA) (Greenbury and Skingle, 1979) and in animal models of collagen-induced arthritis (CIA) (Trentham et al.,

Abbreviations: IFIS, infrared fluorescence imaging system; RA, rheumatoid arthritis; CIA, collagen-induced arthritis; col I, type I collagen; col II, type II collagen; col III, type III collagen; ELISA, enzyme-linked immunosorbent assay; ECL, enhanced chemiluminescence.

* Corresponding author. Tel.: +81 52 853 8204; fax: +81 52 859 1235.
E-mail address: tokamoto@med.nagoya-cu.ac.jp (T. Okamoto).

0022-1759/$ - see front matter © 2005 Elsevier B.V. All rights reserved.
doi:10.1016/j.jim.2005.03.002

1977, 1978). The anti-col II antibody is specific for RA and is not detectable in patients with gout, osteoarthritis and non-arthritic diseases (Fujii et al., 1992). The antibody to native col II was found at highest frequency in early RA, and is associated with active and progressive disease (Cook et al., 1996). Thus, the antibody to col II is useful for early diagnosis of RA and has a predictive value for the disease course. Circulating anti-col II antibody is also found in CIA mice and is considered to be causally associated with arthritis because it was found in the affected articular cartilage as complement-fixing antibodies (Stuart and Dixon, 1983). Moreover, passive transfer of anti-col II antibody could induce arthritis in the recipient mice (Holmdahl et al., 1990; Terato et al., 1992).

Various immunological techniques including a passive hemagglutination assay (Beard et al., 1979), a radioimmunoassay (Clague et al., 1979), and an enzyme-linked immunosorbent assay (ELISA) (Gosslau and Barrach, 1979) have been developed to quantify anti-col II antibodies. These methods differ in sensitivity and specificity (Gosslau and Barrach, 1979; Clague et al., 1983). For example, the passive hemagglutination assay showed high sensitivity but non-specific reactions, causing low specificity, were inevitable as initially indicated (Andriopoulos et al., 1976). Meanwhile, radioimmunoassay has some merits such as high sensitivity and specificity, but the associated radiation hazard and disposal problems are unavoidable (Clague et al., 1979). Although ELISA appeared to have overcome these problems, several concerns have been raised, including the non-specific binding of immunoglobulin to the plastic surface of ELISA plates (Fujii et al., 1989), and contamination of fibronectin, pepsin and proteoglycan in col II preparations (Williams et al., 1992). ELISA has additional disadvantages such as high background levels, high running costs and limited variation of antigens for further analyses, and is therefore unsuitable for research purposes. Some technical improvements in ELISA were attempted including the use of normal rabbit serum to block the non-specific antibody reaction to the plastic plates (Fujii et al., 1989) and extensive purification of col II (Williams et al., 1992). However, even with such modifications the ELISA-based method still suffers from a narrow detection range, as well as high background levels, which limits the accurate quantification of anti-col II antibodies.

In this study, we have applied an immunospot assay system for detecting anti-col II antibodies with an infrared fluorescence imaging system (IFIS), with the secondary antibody labeled Alexa Fluor 680 dye and using a polyvinylidene fluoride (PVDF) membrane. It is well established that IFIS has a number of advantages over ELISA for quantitative detection of antibody reactions such as low background levels and a wide dynamic range (Diggle et al., 2003; Eghbali et al., 2003). The reproducibility and the linearity of this IFIS-based immunospot assay were compared with the conventional immunospot assay using an enhanced chemiluminescence (ECL) detection system. Using this method, our aim was to detect the affinity maturation of anti-col II antibody in the CIA mouse model.

2. Materials and methods

2.1. Antigens

Type II collagen (col II) purified from bovine articular cartilage (catalogue number K41) was purchased from Collagen Research Center (Tokyo, Japan). Type I collagen (col I) (C8919) and type III collagen (col III) (2150-0555) from bovine skin were purchased from Sigma (St. Louis, MO) and Biogenesis (England, UK), respectively. These collagen molecules were highly purified containing less than 0.5% of other protein contaminants (according to the suppliers, other types of collagen amounted to less than 5%). Stock solutions for collagens (typically 0.2 μg/ml) were prepared by dissolving in 0.1 M acetic acid and storing at 4 °C until use.

2.2. Detection of anti-collagen antibody by immunospot assay using IFIS

PVDF membrane (Immobilon-P Transfer membrane, Millipore, Billerica, MA) was pretreated with 99% methanol for 1 min, and washed with transfer buffer (20 mM Tris–HCl (pH 7.4), 150 mM glycine, 20% methanol, 0.005% SDS) for 10 min and rinsed with phosphate buffered saline (PBS). Collagen samples at various concentrations were prepared by diluting the stock solution in PBS and blotted to the pretreated PVDF membrane (100 μl for each well)

using a 96-well dot blot apparatus (Bio-Dot Microfiltration Apparatus; Bio-Rad, CA). The collagen-blotted membrane was washed with PBS three times and each well was blocked with 200 μl of "blocking buffer" (0.03% casein, 0.3% rabbit serum albumin and 0.3% porcine serum albumin in PBS) for 1 h at room temperature. All wells were then washed with PBS containing 1% Tween 20 (PBS/T) four times. Serum samples were diluted with "antibody buffer" (0.1% casein/PBS and 0.01% SDS) at various dilutions (from 1/250 to 1/256,000). For the antibody detection, 100 μl of the serum samples were applied to each well, incubated for 1 h at room temperature, and then all wells were washed with PBS/T four times. The PVDF membrane was detached from the apparatus, and washed with the blocking buffer for 30 min and with PBS/T three times for 20 min each. The membrane was immersed in the secondary antibody solution, Alexa Fluor 680 goat anti-mouse IgG (H and L) (Molecular Probes, Eugene, OR) diluted 1/5000 with the antibody buffer (for one 9 × 12 cm membrane, 1 ml of the 1/5000 diluted secondary antibody solution gave the best results), and incubated for 1 h at room temperature in the dark. The antibody-reacted membrane was sequentially washed with (1) PBS/T three times for 5 min each, (2) PBS/T containing 0.01% SDS for 5 min, and (3) PBS for 15 min. The fluorescence signal (700 nm) emitted from each spot (3.5 mm in diameter) on the membrane was detected using the Odyssey Infrared Imaging System (LI-COR, Lincoln, NE).

2.3. Quantification of anti-collagen antibodies

The Odyssey application software (LI-COR) was used to quantify the infrared fluorescence intensity. In order to quantify the antibody titers, the net intensity of each spot measured by IFIS was found by subtracting the intensity of the background and was defined as the "integrated intensity unit". All measurements were performed in triplicate. Experiments were repeated at least three times.

2.4. Detection and quantification of the anti-collagen antibody by the ECL system

The diluted serum samples and the collagen-blotted PVDF membrane were similarly treated except for the use of another secondary antibody for ECL detection, anti-mouse HRP conjugated immunoglobulin (Amersham Biosciences, Buckinghamshire, UK) diluted to 1/2000 with antibody buffer. After incubating the membrane with 1 ml of the diluted secondary antibody for 1 h at room temperature, the membrane was washed with PBS/T three times for 5 min each and PBS for 15 min. The immunoreactive proteins on the membrane were visualized by ECL using the Super Signal West Pico Chemiluminescent Substrate (Pierce, Rockford, IL) according to the manufacturer's instructions. The membranes were exposed to X-ray film (Bio Max MS Film, Eastmen Kodak, Rochester, NY) and the films were developed using Fluor-S™ MultiImager (Bio-Rad). The densitometric intensity was quantified from each spot (3.5 mm in diameter) on the film by a Multi-Analist/Macintosh software (Bio-Rad). The antibody titer was expressed as densitometric intensity (OD).

2.5. Detection and quantification of the anti-col II antibody by ELISA

In order to compare IFIS and ELISA, we performed the measurements with the same serum samples from the immunized mice using a commercial ELISA kit (Chondrex, Redmond, WA) according to the supplier's protocol. The serum samples were diluted with the sample dilution reagent at various dilutions (from 1/250 to 1/256,000). Briefly, 100 μl of the diluted serum samples were applied to each well and incubated overnight at 4 °C. Then, the secondary antibody (peroxidase-conjugated goat anti-mouse IgG) diluted at 1/2000 was added and incubated for 2 h at room temperature. After washing, all samples were treated with peroxidase reaction solution containing *o*-phenylenediamine and H_2O_2 and incubated for 30 min at room temperature. The reaction was stopped by adding 2.5 N sulfuric acid and the optical density (OD) at 490 nm was measured using a microplate photometer.

2.6. Induction of CIA

DBA/1J ($I\text{-}A^q$) mice at 7–8 weeks of age were purchased from Charles River Laboratories (Yokohama, Japan). They were bred and cared for in a pathogen-free animal facility at Nagoya City University Medical School in accordance with institutional guidelines. For induction of CIA, these mice were

anesthetized with diethyl ether and immunized intradermally at the base of tail and near the axillary and inguinal lymph nodes with 50 μg or 200 μg of bovine col II emulsified with an equal volume of complete Freund's adjuvant (CFA; Difco Laboratories, Detroit, MI) on day 0. On day 21, the mice were boosted with col II in the same manner but using incomplete Freund's adjuvant (IFA; Difco Laboratories). These

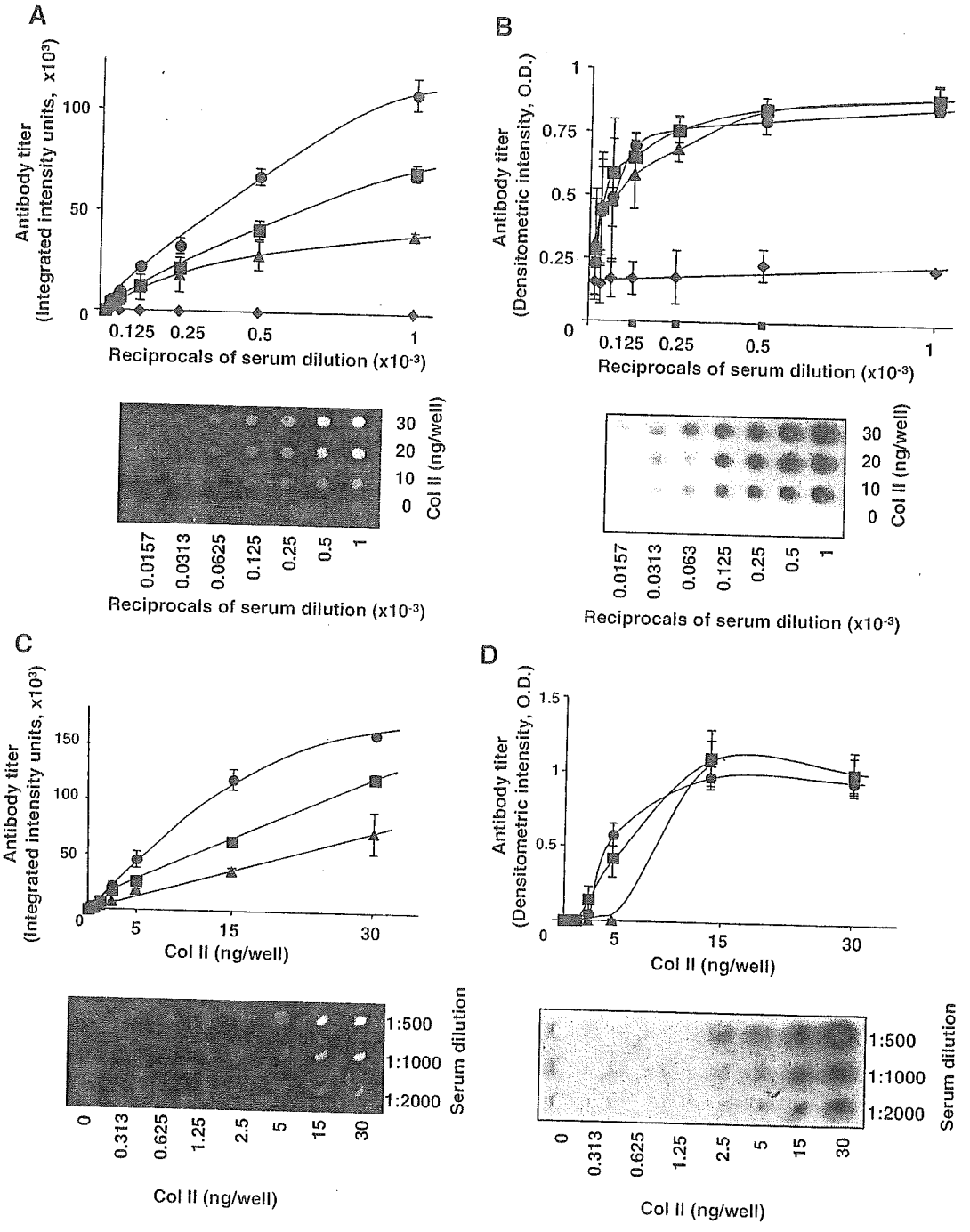

mice developed typical CIA after 4 weeks of primary immunization. Serum samples were collected from three mice immunized with 200 μg of col II on week 5 and used as a standard anti-col II antibody ("CIA serum"). Serum samples used for the evaluation of affinity maturation of antibodies were obtained from four mice immunized with 50 μg of col II on weeks 0, 3, 4, 6 and 14.

2.7. Statistical analysis

All statistical analyses were carried out using the JUSE statistics software package (JUSE-QCAS, version 4.0; Institute of Japanese Union of Scientists and Engineers, Tokyo, Japan). Linear regression analysis was performed to examine the antibody reactivity using the least squares method. The linear relationship was evaluated using the t distribution and considered statistically significant if the calculated t value (t_0) was greater than the statistical t value estimated from the t distribution. To stringently examine the linearity of the antibody measurements for each method, we have adopted the percentage points of the t distribution at $P<0.001$. Validation of each linear regression model was performed using the unbalanced two-way ANOVA. A P value of <0.05 was considered significant.

3. Results

3.1. Comparison of IFIS and ECL methods for the detection of anti-col II antibody

Serum samples were collected and pooled from three CIA mice immunized with col II and used as a standard anti-col II antibody (henceforth, "CIA serum"). To compare IFIS and ECL methods, we carried out these assays on a like-for-like basis using the CIA serum. To determine the optimal antigen concentration for the measurement of anti-col II antibody, various amounts of col II (0, 10, 20 and 30 ng/well) were reacted with the CIA serum at various serum dilutions. As shown in Fig. 1A, linear dose (antibody)–response (measurement) curves were obtained with CIA serum diluted from 1/1000 to 1/64,000 using IFIS. The linearity was evaluated by t distribution test for each amount of the antigen (col II). The calculated t_0 values for 10, 20 and 30 ng/well of col II were 8.3, 32.2 and 30.1, respectively, which are greater than the estimated t value (5.4, $P<0.001$) and considered significant. In contrast, the t_0 values obtained with the ECL detection method for each col II antigen (ng/well) were 3.9, 3.3 and 3.8, and not statistically significant (Fig. 1B). Moreover, the variance of the measurements using the ECL detection method, as depicted by greater standard deviation (SD) values in Fig. 1B, were much greater than using IFIS, particularly at higher serum dilutions, indicating the relative lack of reproducibility. Thus, the IFIS method is considered more appropriate than ECL to measure the anti-col II antibody.

In Fig. 1C and D, the dose–response curves obtained with the IFIS and ECL methods were compared, with various amounts of col II and fixed amounts of antibody (1/500, 1/1000, 1/2000). Obvious linearity was observed with lower CIA serum dilutions using IFIS and partially lost with higher amounts of antibody and antigen, presumably because the detection level reached the plateau (Fig. 1C). The calculated t_0 values for IFIS with each antibody concentration (serum dilution at 1/500, 1/1000 and 1/2000) were 19.2, 44.3 and 13.6, which are greater than the estimated t value (5.4, $P<0.001$) and considered significant. Although the t_0 values obtained with the ECL method for each antibody

Fig. 1. Detection of anti-col II antibody by IFIS and ECL. (A, B) Detection of the antibody with fixed amounts of col II. CIA serum was serially diluted (1/1000, 1/2000, 1/4000, 1/8000, 1/16,000, 1/32,000, and 1/64,000) and reacted with various amounts of col II antigen (●, 30 ng/well; ■, 20 ng/well; ▲, 10 ng/well; ◆, 0 ng/well) blotted on PVDF membrane. Antibody reactivity was detected by IFIS (A) or ECL (B) methods. Note that the IFIS detection with 20 ng col II/well gave the antibody reactivity with highest linearity ($y=39088x+1978$, $P<0.01$ by ANOVA). (C, D) Detection of the anti-col II antibody with fixed amounts of antibody. Fixed amounts of CIA serum (1/500, 1/1000, and 1/2000) were reacted with various amounts of antigen (col II) spotted on PVDF membrane (0, 0.313, 0.625, 1.25, 2.5, 5, 15, and 30 ng/well). Antibody reactivity was detected by IFIS (C) or ECL (D) methods (●, 1/500; ■, 1/1000; ▲, 1/2000). Note that the IFIS detection with 1/1000 dilution of CIA serum gave the antibody reactivity with highest linearity ($y=1997x+7679$, $P<0.01$ by ANOVA). The actual images of the antibody reaction for each experimental condition are shown below each graph. All measurements were performed in triplicate, and all experiments were repeated at least three times. All error bars give standard errors of the mean.

concentration were 8.1, 8.0 12.7 and considered significant, the linearity of the dose–response curves with IFIS were much better than with ECL. In addition, the measurements using the ECL detection method reached a plateau at 15 ng/well of col II even with lower amounts of the antibody (Fig. 1D). Furthermore, the variance in the measurements with ECL were generally much greater than with IFIS. These findings indicate that the IFIS method is more reliable and is better able to quantify anti-col II antibody than the ECL method.

3.2. Further evaluation of the quantitative measurement of anti-col II antibody using IFIS and ELISA

Based on the antibody-antigen reactivity (Fig. 1A), the antigen (col II) amount of 20 ng/well was considered the most appropriate condition for detecting anti-col II antibodies by the IFIS method. We further explored this method using the same experimental conditions described in Fig. 1A with extended dilutions of CIA serum (up to 1/256,000) (Fig. 2A). The linear dose–response relationship ($y=39088x+1978$; $P<0.01$ by unbalanced two-way ANOVA) was obtained. When CIA serum was diluted higher than 1/128,000, the reaction reached a level close to the background (depicted by the reactivity with control sera). The reaction plateau was observed with CIA serum diluted lower than 1/250. Thus, a dynamic range of approximately 500-fold (1/250 to 1/128,000) in detecting anti-col II was estimated using the IFIS method. The very narrow range of SD values in Fig. 2 indicates the reproducibility of this method. Together with the results of Fig. 1C, we used these conditions (antigen, col II 20 ng/well; serum sample, 1/1000 dilution) for further analyses.

In Fig. 2B, the anti-col II antibody titers of the same serum samples were determined by

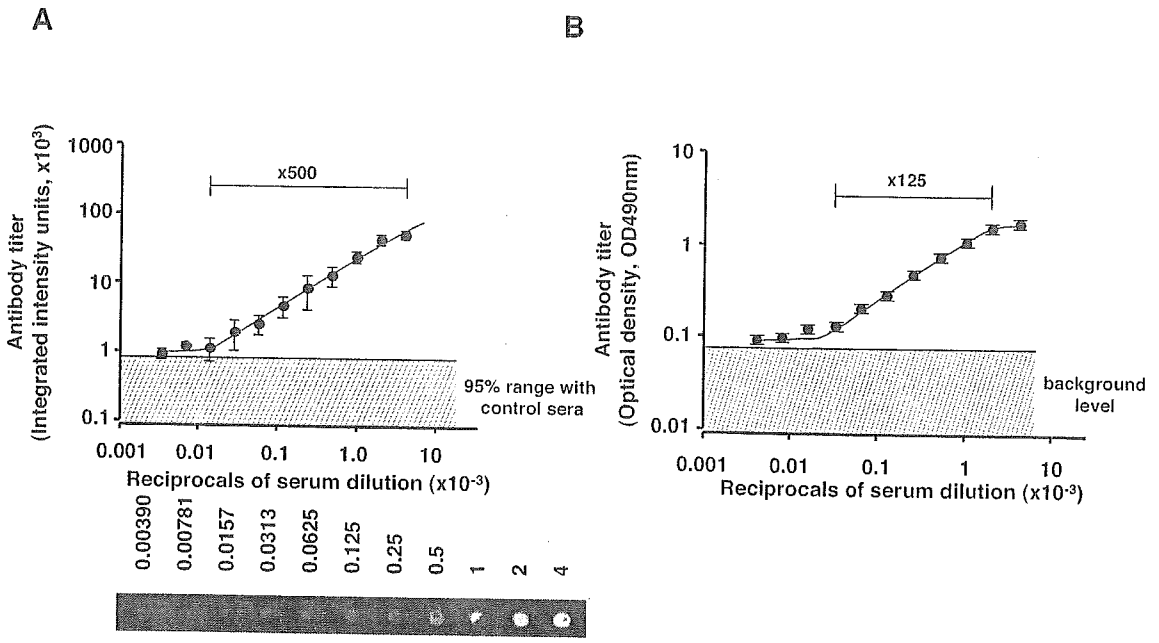

Fig. 2. Evaluation of the quantitative measurement of anti-col II antibody by IFIS and ELISA. (A) Detection of anti-col II antibody by IFIS. A fixed amount (20 ng col II/well) of antigen was spotted on PVDF membrane and the CIA serum was applied at extended dilutions (from 1/250 to 1/256,000). The reactivity plateau appeared when higher amounts of CIA serum (lower than 1/250) were applied. Antibodies greater than 1/128,000 dilutions approached the background level (the 95% range of the reactivity, at 877 integrated intensity units, with control non-immunized sera is shown). The dose–response curve for the antibody–antigen reaction was obtained with significant linearity ($y=39088\,x+1978$, $P<0.01$ by ANOVA). The lower panel shows the image of the anti-col II antibody reaction. (B) Detection of anti-col II antibody by ELISA. The same mouse serum samples (at dilutions from 1/250 to 1/256,000) were used. The dose–response relationship ($y=1.1568\,x+0.1626$; $P<0.01$ by unbalanced two-way ANOVA) was obtained. The dynamic range for detecting anti-col II antibody using each method is indicated.

ELISA. Although a linear dose–response relationship ($y=1.1568x+0.1626$; $P<0.01$ by unbalanced two-way ANOVA) was obtained, the reaction reached a level close to the background when CIA serum was diluted higher than 1/64,000. The reaction plateau was observed with CIA serum diluted lower than 1/500. Thus, the dynamic range in detecting the anti-col II using the ELISA was estimated to be approximately 125-fold (1/500 to 1/64,000) (Fig. 2B). As demonstrated here, the IFIS method was superior to ELISA in that it had higher sensitivity (detection with serum dilution at 1/128,000 for IFIS versus 1/64,000 for ELISA) and a wider dynamic range (500× for IFIS versus 125× for ELISA).

3.3. Antigen specificity of the CIA serum using IFIS

In Fig. 3, we assessed the antigen specificity of the standard CIA serum using the IFIS method. Various dilutions of the CIA and control sera (1/500 to 1/64,000) were reacted with fixed amounts (20 ng/well) of col I, col II and col III. A similar linearity of col II antibody detection was observed as in Fig. 1A. In contrast, only negligible reactivity, close to the background level, was detected using other collagen antigens. Control sera did not react with col II at all. These observations indicate that the IFIS method is useful in detecting anti-col II antibody with high specificity as well as with high sensitivity.

3.4. Affinity maturation of anti-col II antibodies

These features of the IFIS method for anti-col II antibody detection prompted us to explore the affinity maturation process in mice immunized with col II over time. Four mice were immunized with col II (50 μg) and serum samples were collected 0, 3, 4, 6 and 14 weeks after immunization. Antibodies to col I, col II and col III were then measured using IFIS (Fig. 4). Cross-reactive antibodies that reacted with all colla-

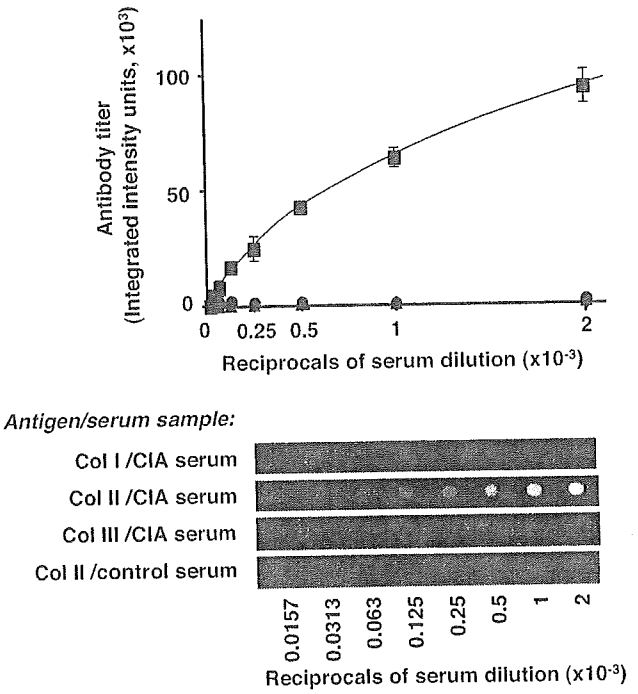

Fig. 3. Antigen specificity of the anti-col II antibody by IFIS. The specificity of anti-col II antibody was assessed by comparing the reactivity with col I, II and III by IFIS. CIA serum and its control were serially diluted (1/500 to 1/64,000) and reacted with 20 ng/well of either col I, col II or col III. Note that no reactivity with col I and col III was detected with CIA serum, even at the highest concentration (1/500 dilution). Control serum did not react with any collagen species at all. ●, col I and CIA serum; ■, col II and CIA serum; ▲, col III and CIA serum; ◆, col II and normal serum. The lower panel illustrates the antibody reactions.

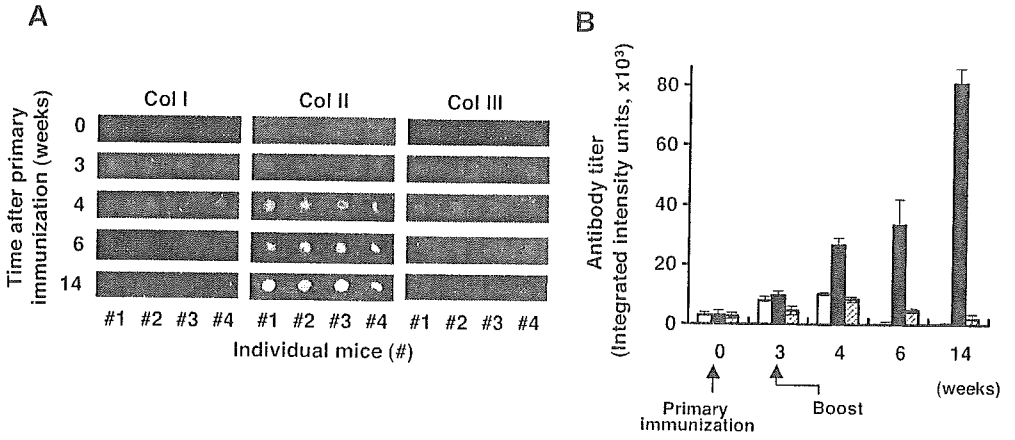

Fig. 4. Detection of the affinity maturation of anti-col II antibodies in CIA mice. (A) The IFIS image of the antibody reactivity following immunization with col II. (B) Quantitative determination of antibody reactivity to col I, col II and col III by IFIS. Serial serum samples were obtained from four mice following immunization with col II (on weeks 0, 3, 4, 6 and 14). The fixed amounts (20 ng/well) of col I, II and III were spotted on PVDF membrane and the antibody reactivity to each collagen antigen was assessed by IFIS with the 1/1000 diluted serum samples obtained from each mouse. Note that serum samples from the immunized mice exhibited cross-reactivity with col I and col II and that the antibody titers of cross-reactive antibodies were diminished over time after the antigen (col II) boost, concomitantly with the elevation of anti-col II antibody titers. Open bars, col I; closed bars, col II; hatched bars, col III.

gen species were detected in earlier stages of immunization. However, the titers of cross-reactive antibodies were gradually diminished after the antigen (col II) boost, concomitantly with the elevation of the anti-col II antibody titers. Thus, the IFIS method was shown to have sufficient specificity and sensitivity to detect the affinity maturation process of the anti-col II antibody in the CIA mouse model.

4. Discussion

In this report, we have developed a new method to detect anti-col II antibody using IFIS. This method enabled us to quantify the antibody with high sensitivity and reproducibility. The dynamic range of antibody measurement reached nearly 500-fold using the optimized conditions. Moreover, we were able to detect the affinity maturation process in mice immunized with col II.

Quantitative measurement of antibodies has been carried out by various methods including passive hemagglutination assay, radioimmunoassay, ELISA, immunoblot, and immunospot assays. As we discussed earlier, ELISA has a number of limitations such as high cost and limited applicability for simultaneous detection of different antigens. Thus, we developed a membrane-based immunospot assay in which col II was spotted on PVDF membrane instead of plastic plates. This technique is similar to the enzyme-linked immunospot assay (Franci et al., 1986). We utilized highly quantitative Alexa Fluor 680 dye and an IFIS detection system (Eghbali et al., 2003; Reeves and Hahn, 2003) for quantification and compared the sensitivity, reproducibility and linearity of the reaction with the conventional immunospot method using ECL detection (Smith et al., 1997).

We found that our IFIS method had a more linear reactivity, having a much broader dynamic range with greater reproducibility than the method using ECL detection (Fig. 1). These differences are considered to be mainly due to the differences in the dynamic ranges of the detection systems. In addition to these advantages, we found that the simplicity of the IFIS method has merit, as the reacted membrane can be immediately subjected to quantification, without any enzymatic reaction or tedious film-exposure and development. In addition, we found that IFIS has higher sensitivity and a wider dynamic range even compared with ELISA (Fig. 2).

The IFIS method enabled us to detect temporal change in antibody specificity in mice immunized with col II. Although we did not examine the

increase in the affinity of antibodies to col II, the gradual loss of antibody reactivity to other collagens, together with the increase in specific reactivity to col II, suggested an affinity maturation process (Shimizu et al., 2003, 2004). These findings indicate a possible application for the analysis of the temporal profile of anti-col II antibody during the clinical course of RA. Although anti-col II antibodies are considered to play an important role in the progression of RA (Tarkowski et al., 1989; Corrigall and Panayi, 2002), the reported prevalence of anti-col II antibodies in RA patients is highly variable (3–80%) (Greenbury and Skingle, 1979; Beard et al., 1980; Fujii et al., 1992; Morgan et al., 1993; Cook et al., 1996). The lack of specificity and sensitivity of the methodology and bias in patient selection could be the reasons for these discrepancies, and may have precluded further analyses. Use of a reliable method, such as demonstrated in this study, should uncover the role of anti-col II antibodies in RA. Furthermore, based on our observations, the IFIS method can also be utilized for the analysis of immunopathological processes in other diseases.

Acknowledgments

We thank Y. Otsuka for helpful technical advice. This work was supported by grants-in-aid from the Ministry of Health, Labor and Welfare, and Ministry of Education, Culture, Sports, Science and Technology.

References

Andriopoulos, N.A., Mestecky, J., Miller, E.J., Bradley, E.L., 1976. Antibodies to native and denatured collagens in sera of patients with rheumatoid arthritis. Arthritis Rheum. 19, 613.

Beard, H.K., Lea, D.J., Ryvar, R., 1979. Anomalous reactions in the haemagglutination assay for anti-collagen antibodies: studies on patients with rheumatoid arthritis or chronic low back pain. J. Immunol. Methods 31, 119.

Beard, H.K., Ryvar, R., Skingle, J., Greenbury, C.L., 1980. Anti-collagen antibodies in sera from rheumatoid arthritis patients. J. Clin. Pathol. 33, 1077.

Clague, R.B., Brown, R.A., Weiss, J.B., Holt, P.J., 1979. Solid-phase radioimmunoassay for the detection of antibodies to collagen. J. Immunol. Methods 27, 31.

Clague, R.B., Firth, S.A., Holt, P.J., Skingle, J., Greenbury, C.L., Webley, M., 1983. Serum antibodies to type II collagen in rheumatoid arthritis: comparison of 6 immunological methods and clinical features. Ann. Rheum. Dis. 42, 537.

Cook, A.D., Rowley, M.J., Mackay, I.R., Gough, A., Emery, P., 1996. Antibodies to type II collagen in early rheumatoid arthritis. Correlation with disease progression. Arthritis Rheum. 39, 1720.

Corrigall, V.M., Panayi, G.S., 2002. Autoantigens and immune pathways in rheumatoid arthritis. Crit. Rev. Immunol. 22, 281.

Diggle, C.P., Bentley, J., Kiltie, A.E., 2003. Development of a rapid, small-scale DNA repair assay for use on clinical samples. Nucleic Acids Res. 31, e83.

Eghbali, M., Toro, L., Stefani, E., 2003. Diminished surface clustering and increased perinuclear accumulation of large conductance Ca^{2+}-activated K^{+} channel in mouse myometrium with pregnancy. J. Biol. Chem. 278, 45311.

Franci, C., Ingles, J., Castro, R., Vidal, J., 1986. Further studies on the ELISA-spot technique. Its application to particulate antigens and a potential improvement in sensitivity. J. Immunol. Methods 88, 225.

Fujii, K., Tsuji, M., Murota, K., Terato, K., Shimozuru, Y., Nagai, Y., 1989. An improved enzyme-linked immunosorbent assay of anti-collagen antibodies in human serum. J. Immunol. Methods 124, 63.

Fujii, K., Tsuji, M., Kitamura, A., Murota, K., 1992. The diagnostic significance of anti-type II collagen antibody assay in rheumatoid arthritis. Int. Orthop. 16, 272.

Gosslau, B., Barrach, H.J., 1979. Enzyme-linked immunosorbent microassay for quantification of specific antibodies to collagen type I II, III. J. Immunol. Methods 29, 71.

Greenbury, C.L., Skingle, J., 1979. Anti-cartilage antibody. J. Clin. Pathol. 32, 826.

Holmdahl, R., Jansson, L., Larsson, A., Jonsson, R., 1990. Arthritis in DBA/1 mice induced with passively transferred type II collagen immune serum. Immunohistopathology and serum levels of anti-type II collagen auto-antibodies. Scand. J. Immunol. 31, 147.

Morgan, K., Clague, R.B., Reynolds, I., Davis, M., 1993. Antibodies to type II collagen in early rheumatoid arthritis. Br. J. Rheumatol. 32, 333.

Reeves, W.M., Hahn, S., 2003. Activator-independent functions of the yeast mediator sin4 complex in preinitiation complex formation and transcription reinitiation. Mol. Cell. Biol. 23, 349.

Shimizu, T., Oda, M., Azuma, T., 2003. Estimation of the relative affinity of B cell receptor by flow cytometry. J. Immunol. Methods 276, 33.

Shimizu, T., Kozono, Y., Kozono, H., Oda, M., Azuma, T., 2004. Affinity maturation of secreted IgM pentamers on B cells. Int. Immunol. 16, 675.

Smith, D., Proctor, S.D., Mamo, J.C., 1997. A highly sensitive assay for quantitation of apolipoprotein B48 using an antibody to human apolipoprotein B and enhanced chemiluminescence. Ann. Clin. Biochem. 34 (Pt. 2), 185.

Stuart, J.M., Dixon, F.J., 1983. Serum transfer of collagen-induced arthritis in mice. J. Exp. Med. 158, 378.

Tarkowski, A., Klareskog, L., Carlsten, H., Herberts, P., Koopman, W.J., 1989. Secretion of antibodies to types I and II collagen by

synovial tissue cells in patients with rheumatoid arthritis. Arthritis Rheum. 32, 1087.
Terato, K., Hasty, K.A., Reife, R.A., Cremer, M.A., Kang, A.H., Stuart, J.M., 1992. Induction of arthritis with monoclonal antibodies to collagen. J. Immunol. 148, 2103.
Trentham, D.E., Townes, A.S., Kang, A.H., 1977. Autoimmunity to type II collagen: an experimental model of arthritis. J. Exp. Med. 146, 857.
Trentham, D.E., Townes, A.S., Kang, A.H., David, J.R., 1978. Humoral and cellular sensitivity to collagen in type II collagen-induced arthritis in rats. J. Clin. Invest. 61, 89.
Williams, R.O., Williams, D.G., Maini, R.N., 1992. Anti-type II collagen ELISA. Increased disease specificity following removal of anionic contaminants from salt-fractionated type II collagen. J. Immunol. Methods 147, 93.

Inhibition of the 53BP2S-mediated apoptosis by nuclear factor κB and Bcl-2 family proteins

Naoko Takahashi[1], Shinya Kobayashi[1], Shinichi Kajino[1], Kenichi Imai[1], Keisuke Tomoda[1], Shigeomi Shimizu[2] and Takashi Okamoto[1,*]

[1]*Department of Molecular and Cellular Biology, Nagoya City University Graduate School of Medical Sciences, 1 Kawasumi, Mizuho-cho, Mizuho-ku, Nagoya, Aichi 467-8601, Japan*

[2]*Laboratory of Molecular Genetics, Osaka University Medical School, 2-2 Yamadaoka, Suita, Osaka 565-0871, Japan*

The p53 binding protein 2 (53BP2) has been identified independently as the interacting protein to p53, Bcl-2, and p65 subunit of nuclear factor κB (NF-κB). It was demonstrated that over-expression of 53BP2 (renamed as 53BP2S) induces apoptotic cell death. In this study we explored the effect of NF-κB activation elicited by a physiological NF-κB inducer, interleukin-1β (IL-1β), and anti-apoptotic Bcl-2 family proteins on the 53BP2S-mediated apoptosis. We found that both NF-κB activation and Bcl-2 family proteins could prevent the 53BP2S-mediated depression of mitochondrial transmembrane potential, activation of caspase-9, cleavage of poly ADP ribose polymerase (PARP), and cell death. These observations suggested that 53BP2S/Bbp and its directly or indirectly interacting proteins might play crucial roles in the regulation of apoptosis and contribute to carcinogenesis. It is also suggested that 53BP2S/Bbp induces apoptosis through the mitochondrial death pathway presumably by counteracting the actions of anti-apoptotic Bcl-2 family proteins. The regulatory network of the 53BP2S-mediated apoptosis cascade including its interacting proteins is discussed.

Introduction

Although the p53 binding protein 2 (53BP2) was identified as one of the interacting proteins to p53 (Iwabuchi *et al.* 1994), subsequent studies found that it also interacts with Bcl-2 (Naumovski & Cleary 1996) and p65 subunit of nuclear factor κB (NF-κB) (Yang *et al.* 1999), suggesting its role in carcinogenesis. We recently found that although the 53BP2 protein is encoded by a single copy gene *TP53BP2* located in the long arm of chromosome 1 at q42.1 (Yang *et al.* 1997), two isoform proteins, 53BP2S and 53BP2L, formerly named 53BP2 (Yang *et al.* 1999) or Bcl-2 binding protein (Bbp) (Naumovski & Cleary 1996) and ASPP2 (Samuels-Lev *et al.* 2001), respectively, are generated by alternative splicing (Takahashi *et al.* 2004). We and others reported the proapoptotic action of 53BP2S/Bbp by demonstrating the annexin V staining, nuclear fragmentation, and induction of cell death (Yang *et al.* 1999; Lopez *et al.* 2000; Ao *et al.* 2001; Samuels-Lev *et al.* 2001; Bergamaschi *et al.* 2004). In addition, we have recently found that 53BP2S/Bbp is translocated to the mitochondria and induces cell death through the mitochondrial death pathway (Kobayashi *et al.* 2005).

53BP2 proteins interact with p53, p65 and Bcl-2 through the C-terminal ankyrin repeats and SH3 domain (Iwabuchi *et al.* 1994; Naumovski & Cleary 1996; Yang *et al.* 1999). Previous studies indicated that the 53BP2 binding site in the p53 core domain is evolutionarily conserved and is frequently mutated in human cancer (Iwabuchi *et al.* 1994; Gorina & Pavletich 1996), suggesting that 53BP2 proteins may participate in the biological actions of p53. In fact, we found that the levels of 53BP2 mRNA expression in various human cancer cell lines was correlated with the sensitivity to DNA damaging agents irrespectively of the p53 status (Mori *et al.* 2000), indicating the biological relevance *in vivo*.

In this study, we have further explored the effects of NF-κB and Bcl-2 family proteins on the proapoptotic action of 53BP2S/Bbp. We found that both NF-κB and Bcl-2 family proteins could prevent the 53BP2S-mediated apoptosis. The biological roles of 53BP2 proteins and these interacting proteins in the regulation of apoptosis, and their possible roles in carcinogenesis are discussed.

Communicated by: Hideyuki Okano

**Correspondence*: E-mail: tokamoto@med.nagoya-cu.ac.jp

DOI: 10.1111/j.1365-2443.2005.00878.x

Results

Induction of apoptosis by 53BP2S

To assess the proapoptotic effect of 53BP2S/Bbp, we transfected 53BP2S gene in MIA PaCa-2 cells and the induction of apoptosis was evaluated by typical nuclear morphology and trypan blue dye exclusion assay. In Fig. 1A, when MIA PaCa-2 cells were transfected with pEGFP-53BP2 (Yang *et al.* 1999), expressing 53BP2S/Bbp, the typical apoptotic morphology, such as nuclear condensation and fragmentation, was observed in these transiently transfected cells. Approximately 32% of cells exhibited apoptosis when 53BP2S was transduced, which was significantly higher than the control (6.2%; $P < 0.01$) (Fig. 1B). To further confirm the effect of 53BP2S/Bbp, 293/53BP2 cells, a stable cell line in which 53BP2S/Bbp expression is under the stringent control of ponasteron A (pon A), were treated with pon A to induce 53BP2S/Bbp expression. After 24 h of postinduction, similar apoptotic nuclear changes were observed in 293/53BP2 cells whereas the control 293/LZ cells did not show such changes (Fig. 1C). In Fig. 1D, the number of surviving cells in 293/53BP2 and 293/LZ cultures were counted by trypan blue dye exclusion assay,

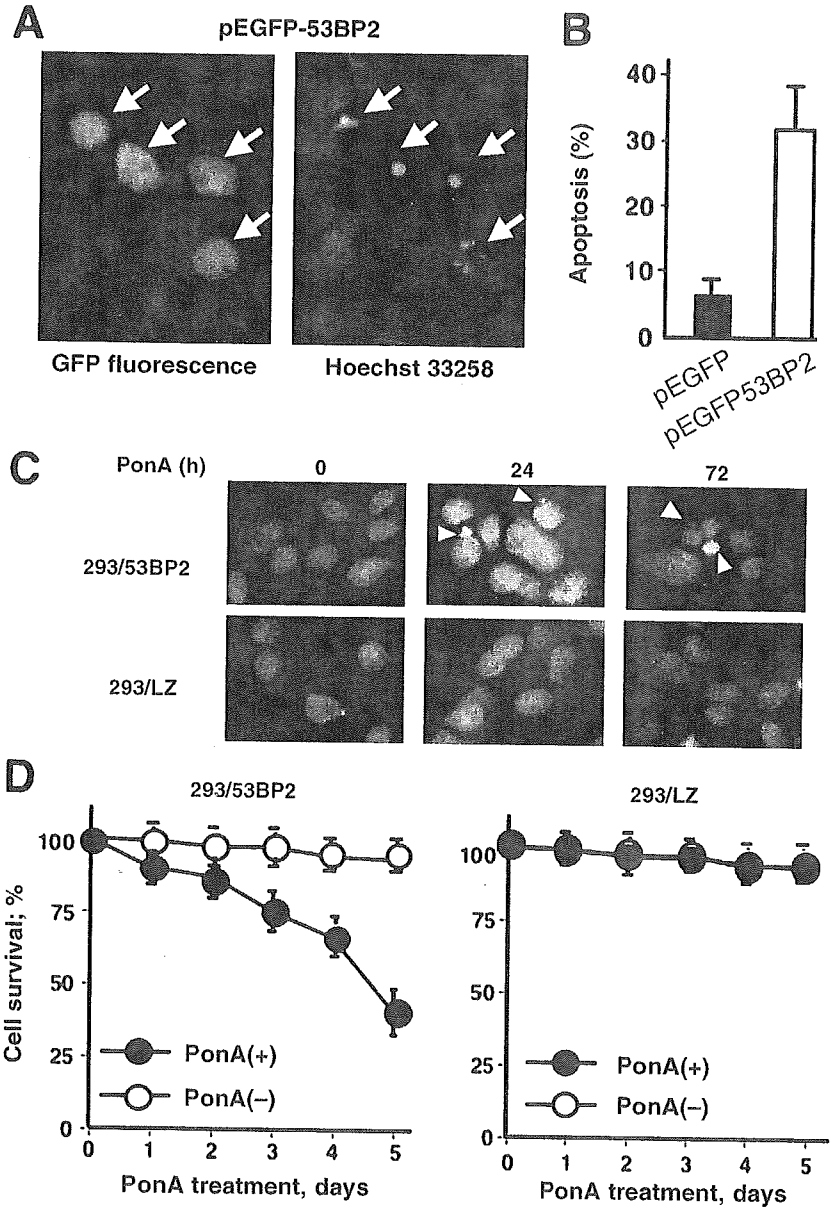

Figure 1 Induction of apoptosis by 53BP2S protein. (A) Nuclear morphology of 53BP2S-transfected cells. MIA PaCa-2 cells were transfected with pEGFP-53BP2, stained with Hoechst 33258, and observed under a fluorescence microscope. Arrows indicate the locations of transfected cells with typical nuclear morphology of apoptotic cells. (B) Quantification of the proapoptotic effect of 53BP2S. The percentage of apoptotic cells among the GFP stained cells is shown. ■ transfection with pEGFP (control); □ transfection with pEGFP-53BP2. (C) Nuclear morphology of apoptotic cells in 293/53BP2 upon 53BP2S/Bbp induction. The pon A-induced cells were stained with Hoechst-33258 and observed under a fluorescent microscopy. The apoptotic cells were identified by their fragmented and/or condensed nuclear morphology (indicated by arrowheads). (D) Induction of cell death by 53BP2S/Bbp. 293/53BP2 and 293/LZ (control) cells were stimulated with pon A (5 μM) for the indicated periods (in days) and stained with trypan blue. The surviving cells, not stained with trypan blue, were counted.

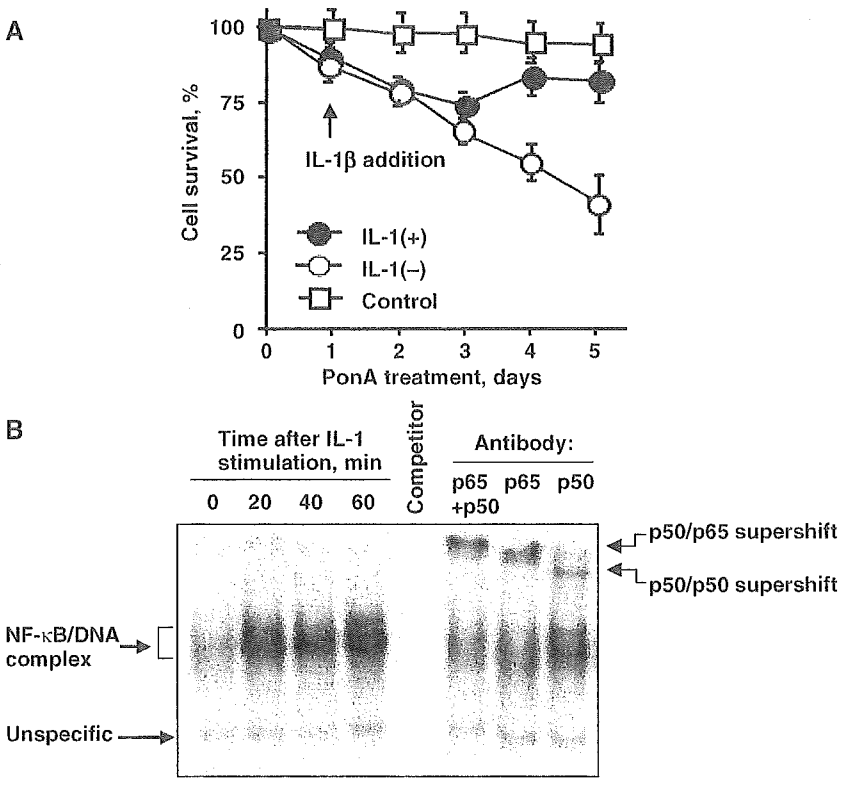

Figure 2 Inhibition of the 53BP2S-induced cell death by the treatment with IL-1β. (A) 293/53BP2 cells were treated with pon A (5 μM) and NF-κB was activated by IL-1β (20 ng/mL) after 1 day of pon A treatment. Cell survival rate was assessed by dye exclusion assay using trypan blue. After pon A treatment, cells were either stimulated with (●) or without IL-1β (○). Control (□), 293/53BP2 cells without pon A treatment. (B) Activation of NF-κB DNA-binding activity. 293/53BP2 cells were simulated with IL-1β (20 ng/mL) for indicated time periods and were harvested to prepare the nuclear extract for EMSA with the κB DNA probe. Supershift assays were performed by incubating the nuclear extract (40 min after IL-1β stimulation) with polyclonal antibodies against p65 and p50.

with or without pon A, over time following the induction. The survival rate of 293/53BP2 cells decreased upon 53BP2S/Bbp expression and reached 54%, whereas that of the untreated cells (without pon A) was only 3%, and was similar to the background level of control cells (293/LZ).

Inhibition of the 53BP2S-induced cell death by NF-κB activation

To examine the effect of NF-κB activation on the 53BP2S-induced cell death, IL-1β was added after the production of 53BP2S protein by ponA treatment for 24 h in 293/53BP2 cells. As shown in Fig. 2A, the 53BP2S-mediated cell death was prevented. There was a time lag of approximately 48 h between the addition of IL-1β and the appearance of inhibition of cell death. In the experiment demonstrated in Fig. 2A, 53(B)P2S protein was detectable after 12 h ponA treatment (data not shown). The NF-κB activation by IL-1β was monitored by the induction of its DNA binding activity as demonstrated by the electrophoretic mobility shift assay (EMSA) (Fig. 2B). Whereas the cell survival rate of the 53BP2S-expressing cells was 42% after 5 days of pon A treatment, that of the cells treated with IL-1β (24 h after the pon A treatment) exhibited an 84% survival rate, which was very close to the level of control 293/LZ cells not expressing 53BP2S/Bbp (Fig. 2A). The IL-1β treatment had no effect on the level of 53BP2S/Bbp expression *per se* in 293/53BP2 cells (data not shown). In addition, we detected expression of Bcl-2 and Bcl-X_L proteins and their levels were not further up-regulated by the IL-1β treatment (data not shown).

As shown in Fig. 3, the 53BP2S-induced cell death was associated with the cleavage of poly ADP ribose polymerase (PARP), a typical biochemical marker of apoptosis. It is also shown that the cleaved form of caspase-9 at 24 h after ponA treatment, but not caspase-8, was emerged, suggesting that the 53BP2S/Bbp induces cell death through the mitochondrial death pathway. No such changes were detected in the control 293/LZ cells (data not shown). However, when 293/53BP2 cells were treated with IL-1β, the PARP cleavage and the emergence of caspase-9 were prevented.

Inhibition of the 53BP2S-mediated apoptosis by Bcl-2 and Bcl-X_L

We then examined the effect of Bcl-2 family proteins on the 53BP2S-mediated apoptosis. Bcl-2, Bcl-X_L, and ΔBH4 mutant of Bcl-X_L lacking the crucial BH4 domain, were

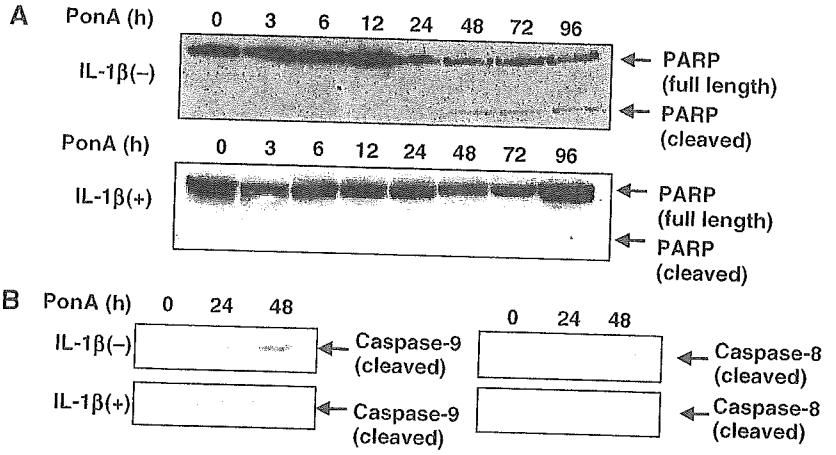

Figure 3 Inhibition of the 53BP2S-induced PARP cleavage by IL-1β treatment. (A) 293/53BP2 cells were pretreated with or without IL-1β (20 ng/mL) for 12 h and 53BP2S/Bbp expression was induced by pon A (5 μM). These cells were harvested for the examination of PARP cleavage by Western blotting with anti-PARP rabbit polyclonal antibody. The positions of the intact full-length PARP (116 kDa) and its cleaved form (89 kDa) are indicated by the arrows. Experiments were repeated three times and the same results were obtained. (B) Inhibition of caspase-9 activation by IL-1β. Pretreatment of 293/53BP2 cells with IL-1β and induction of 53BP2S/Bbp were similarly performed as above. The position of the activated ('cleaved') form of caspase-9 is indicated by the arrow. No activation of caspase-8 was detected by 53BP2 induction.

expressed together with 53BP2S/Bbp in MIA PaCa-2 cells and the number of apoptotic cells were counted. As shown in Fig. 4, both Bcl-2 and Bcl-X_L expression inhibited 53BP2S-induced cell death in a dose-dependent manner, with greater inhibitory effect of Bcl-X_L. No such effect was observed with ΔBH4 mutant.

Since these anti-apoptotic Bcl-2 proteins are known to block cell death by restoring the mitochondrial membrane potential ($\Delta\Psi m$), we examined $\Delta\Psi m$ of the transfected cells by staining with a fluorescence dye CMX-ROS (Fig. 5). Whereas 53BP2S/Bbp induced the reduction of $\Delta\Psi m$, observed by the reduction of mitochondrial staining with CMX-ROS, expression of Bcl-2 or Bcl-X_L, but not ΔBH4 mutant, prevented its reduction. These results confirmed the anti-apoptotic effect of anti-apoptotic Bcl-2 proteins shown in Fig. 4.

Discussion

The present data have revealed the inhibitory effects of NF-κB and Bcl-2 family proteins on the 53BP2S-mediated apoptosis. The partial clone of 53BP2 was initially identified as one of the interacting proteins of p53 (Iwabuchi *et al.* 1994). Since NF-κB p65 subunit and Bcl-2 are known to inhibit apoptosis (DeLuca *et al.* 1998; Haddad 2004) and have previously been reported to interact with 53BP2S/Bbp (Naumovski & Cleary 1996; Yang *et al.* 1999), our findings indicate that anti-apoptotic actions of these proteins appear to be through blocking the pro-apoptotic actions of 53BP2S/Bbp at least in a part. Thus, 53BP2S-mediated apoptosis is regulated by p53, NF-κB and Bcl-2/Bcl-X_L (Fig. 6).

Because of its localization and negative regulation by anti-apoptotic Bcl-2 family proteins, it is suggested that 53BP2S/Bbp induces apoptosis by stimulating the effect of intrinsic (mitochondrial) death pathway mediated by proapoptotic Bcl-2 family proteins or by blocking the actions of anti-apoptotic Bcl-2 family proteins. Since 53BP2S/Bbp is known to interact with Bcl-2 at least *in vitro* as well as in yeast cells (Naumovski & Cleary 1996), and Bcl-X_L and Bcl-2 exhibit a high structural and functional similarity, it is possible that 53BP2S/Bbp can interfere with actions of these anti-apoptotic Bcl-2 family proteins. However, we and others failed to detect the protein–protein interaction of 53BP2S/Bbp and these Bcl-2 proteins in cells (data not shown). Thus, further studies are needed to address this possibility. From experimental observations so far obtained, we speculate that 53BP2 may down-modulate the cell death 'rheostat' (Daniel & Korsmeyer 2004), that is maintained by the balance between pro-apoptotic and anti-apoptotic Bcl-2 proteins (Haddad 2004) and set the threshold of susceptibility to apoptosis, by blocking the action of anti-apoptotic Bcl-2 family proteins at the vicinity of mitochondria (Fig. 6).

It is not clear whether p53 is required for the proapoptotic action of 53BP2 proteins. Lopez *et al.* (2000) observed that the DNA damage induced the 53BP2S/

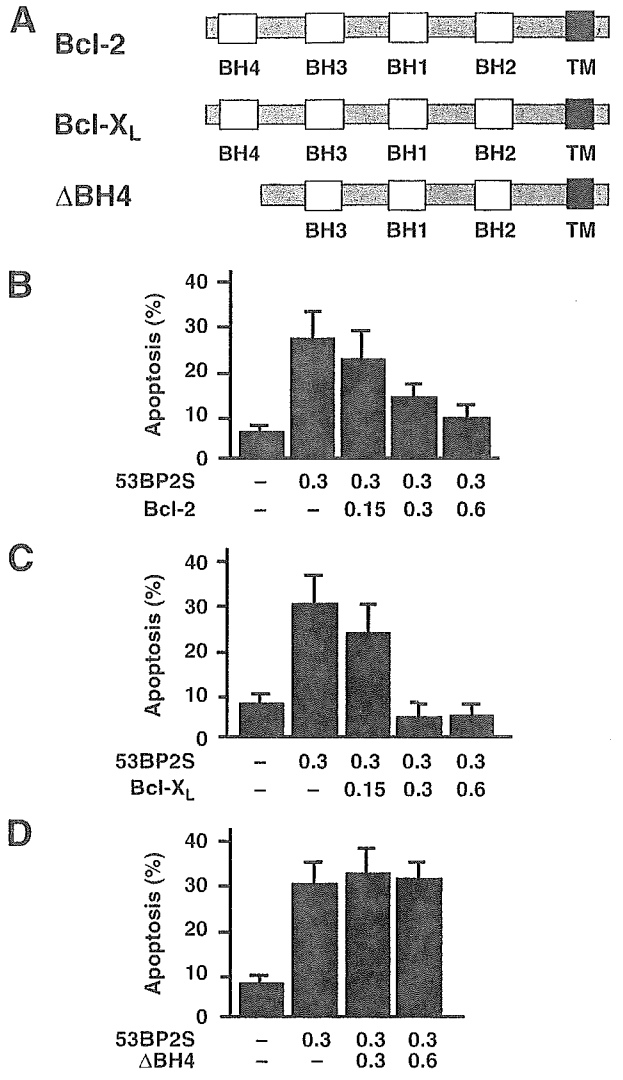

Figure 4 Attenuation of 53BP2S-induced apoptosis by Bcl-2 and Bcl-X_L. (A) The schematic representation of Bcl-2 proteins used in this study. (B, C, D) Effects of Bcl-2 proteins on the 53BP2S-mediated apoptosis. MIA PaCa-2 cells were transfected with pcDNA3.1-53BP2, expressing 53BP2S/Bbp, together with pCAGGA-Bcl-2, pCAGGA-Bcl-X_L or pCAGGA–ΔBH4, and apoptotic cells were counted. The average and the S.D. values of four independent experiments are shown. Note that no effect was observed with the Bcl-X_L mutant (ΔBH4). The amounts (μg) of each plasmid are indicated.

Bbp expression and protein stabilization leading to apoptosis in the context of wild-type p53, although p53 suppressed 53BP2S/Bbp expression in undamaged cells. We and others have previously reported very low 53BP2 protein levels in spite of the highly abundant mRNA and suggested a possibility that the 53BP2 level might be regulated at the post-translational level (Naumovski & Cleary 1996; Yang *et al.* 1999; Lopez *et al.* 2000). Thus, the p53 interaction may stabilize 53BP2 proteins and enhance its apoptotic action. In addition, it was reported that p53-mediated transactivation was augmented by 53BP2S/Bbp (Iwabuchi *et al.* 1998) and 53BP2L/ASPP2 (Samuels-Lev *et al.* 2001). Samuels-Lev *et al.* (2001) proposed a model in which 53BP2L/ASPP2 interacts with p53 in the nucleus and specifically enhances gene expression of p53 responsive proapoptotic genes such as Bax. However, although MIA PaCa-2 cells contain p53 mutation at R248 (Yoshikawa *et al.* 1999), known to be involved in the interaction with 53BP2 at least in a crystal structure of the p53–53BP2 protein complex (Gorina & Pavletich 1996), we found that 53BP2S/Bbp could induce apoptosis in MIA PaCa-2 cells much more efficiently than in 293 cells, expressing wild-type p53 (Fig. 1). Thus, it is yet to be investigated whether 53BP2-mediated apoptosis requires the interaction with p53 and whether 53BP2S/Bbp and 53BP2L/ASPP2 have distinct actions in cells. It is also possible that proapoptotic actions of 53BP2 proteins are exerted at multiple levels.

We confirmed the inhibitory effect of NF-κB activation on the proapoptotic action of 53BP2S/Bbp. We demonstrate that anti-apoptotic action of NF-κB was evident even after the initiation of 53BP2S-mediated cell death (Fig. 2). The anti-apoptotic nature of NF-κB has been well established (DeLuca *et al.* 1998; Chen *et al.* 2001; Karin & Lin 2002). There are at least two mechanisms by which NF-κB inhibits apoptosis: (i) by induction of gene expression of anti-apoptotic proteins such as c-IAP2 (Chu *et al.* 1997), IEX-1 L (Wu *et al.* 1998) and even Bcl-X_L (Chen *et al.* 2000) and (ii) through blocking the action of proapoptotic factors by direct or indirect interaction (Yang *et al.* 1999). However, these two distinct mechanisms are not mutually exclusive for neither one mechanism alone can fully explain the strong anti-apoptotic action of NF-κB. In suppor of the latter mechanism, we observed that NF-κB could inhibit the TNF-α-mediated apoptosis without *de novo* protein synthesis at least in some cell lines (Kajino *et al.* 2000). Although the intracellular location where NF-κB interacts with 53BP2S/Bbp is not known, it may occur in the vicinity of mitochondria since NF-κB and IκBα are found in the mitochondrial intermembrane space and TNF-α can liberate the NF-κB within mitochondria (Bottero *et al.* 2001; Cogswell *et al.* 2003). Thus, 53BP2S/Bbp could serve as one of the molecular targets for the anti-apoptotic actions of NF-κB. However, since the delay of the anti-apoptotic effect of IL-1β on 53BP2S-mediated apoptosis was observed, it is possible that both

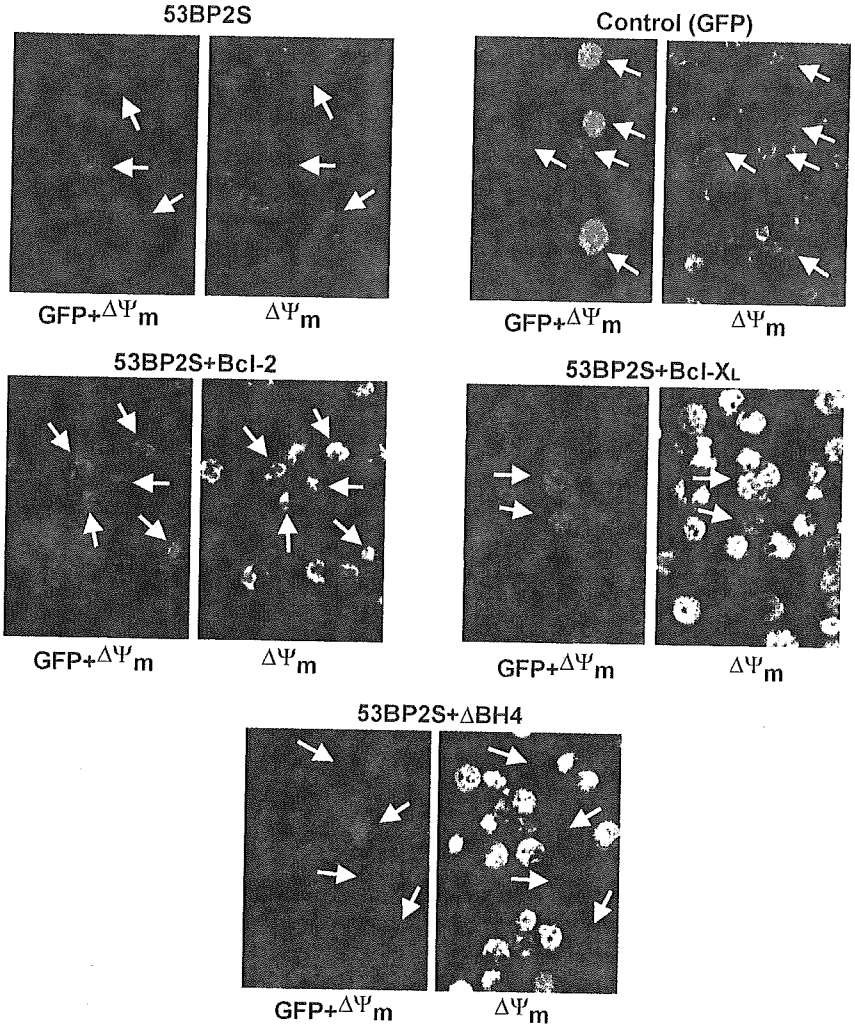

Figure 5 Restoration of ΔΨm depression on 53BP2S induction by Bcl-2 or Bcl-X_L. MIA PaCa-2 cells were transfected with pEGFP- 53BP2 or pEGFP (control). Effects of co-transfection with pUC-CAGGS-Bcl-2, pUC-CAGGS-Bcl-X_L or pUC-CAGGS-ΔBH4 were examined. Twenty-eight hours after the transfection, the cells were stained with CMX-ROS and the Δψm was observed under the confocal microscope. Figures on the left represent merged images of GFP (53BP2S/Bbp) staining (green) and CMX-ROS (Δψm) staining (red) and those on the right represent the CMX-ROS fluorescence on the right for clarity. Arrows indicate the locations of transfected (GFP-stained) cells. All figures were viewed in the same conditions (CMX-ROS concentration, fixation procedure, and exposure time for microscopic examination).

direct and indirect effects of NF-κB actions are involved in 53BP2S-induced apoptosis.

These observations have indicated the role of NF-κB in various pathologies and implicated NF-κB as a common therapeutic target (Karin & Lin 2002). For example, Arlt *et al.* (2002) reported that the blockade of NF-κB activation cascade by its inhibitors MG132 and sulfasalazine greatly augmented the effect of doxorubicin or etoposide in inducing the cell death of human pancreatic cancer cell lines. Use of these compounds and derivatives is expected to augment the therapeutic efficacy of conventional cancer therapy.

These findings support a possibility that 53BP2 proteins are involved in various biological processes such as carcinogenesis and the cellular response to DNA damage. Mori *et al.* (2000) reported that the level of 53BP2 mRNA expression in various human cancer cell lines was correlated with the sensitivity to DNA damaging agents although no mutation of 53BP2 gene was detected. In addition, Ao *et al.* (2001) observed that 53BP2S/Bbp expression augmented the cellular apoptotic response to the DNA damage. Thus, selective action of 53BP2 with p53, Bcl-2 and NF-κB p65 subunit may determine the susceptibility of cells to trigger the apoptotic pathway in response to the DNA damage (Fig. 6).

Experimental procedures

Reagents and antibodies

Human recombinant cytokine IL-1β (Boehringer Mannheim, Mannheim, Germany), Hoechst-33258 (Molecular Probes, Eugene, OR, USA), CMX-ROS (Molecular Probes), Ponasterone A (pon A) (Invitrogen, La Jolla, CA, USA) were commercially obtained. SuperFect transfection reagents was purchased from QIAGEN (Qiagen Inc., Valencia, CA, USA). Mouse monoclonal antibodies to human 53BP2 proteins (BD Transduction Laboratories,